In: 2024 IEEE International Workshop on Technologies for Defense and Security (TechDefense),
11-13 November 2024, Naples, Italy
DOI:10.1109/techdefense63521.2024.10863447

A Cognitive-Based ISAR System for Spectral Compatibility Applications

Massimo Rosamilia[1,2], Augusto Aubry[1,2], Alessio Balleri[3], Antonio De Maio[1,2], and Marco Martorella[1,4]
[1]National Inter-University Consortium for Telecommunications, Parma, Italy
[2]Department of Electrical Engineering and Information Technology,
University of Naples "Federico II", I-80125 Naples, Italy
[3]Centre for Electronic Warfare, Information and Cyber,
Cranfield University, Defence Academy of the United Kingdom, Shrivenham, SN6 8LA, United Kingdom
[4]Department of Electronic, Electrical and Systems Engineering,
University of Birmingham, B15 2TT Birmingham, U.K.

***Abstract*—This paper proposes and analyzes the concept of a cognitive inverse synthetic aperture radar (ISAR) ensuring spectral compatibility in crowded electromagnetic environments. In such a context, cognitive radar system alternates between a perception stage, recognizing possible emitters in its frequency range, and an action stage, synthesizing and transmitting a tailored radar waveform to achieve the desired task while guaranteeing the spectral coexistence with overlaid emitters. The perception stage is carried out by an electronic support measurement system (ESM) that senses the environment and extracts relevant spectral parameters. The action stage employs a tailored signal design process, synthesizing a radar waveform with bespoke spectral notches, enabling ISAR imaging over a wide spectral bandwidth without interfering with the other radio frequency (RF) systems. A key enabling technology for the proposed application is the compressed sensing (CS) framework, allowing accurate ISAR imaging even with missing data in the frequency domain (induced by spectral notches) and in the slow-time dimension (enabling the system to perform additional RF activities). The capabilities of the proposed system are assessed exploiting a dataset of drone measurements in the frequency band $[13, 15]$ GHz. The results highlight the effectiveness of the proposed system to enable the spectral compatibility while delivering high-quality ISAR images.**

***Index Terms*—ISAR, cognitive radar, compressed sensing, spectral compatibility, drone detection, missing data**

I. Introduction

The electromagnetic spectrum is a valuable and highly dynamic resource that is often inadequately exploited by contemporary radar systems [1]. Accordingly, an essential requirement for a next-generation radar system is the ability to work in a congested electromagnetic spectrum, guaranteeing compatibility with overlaid emitters while better exploiting the available frequency intervals. Recent research emphasizes the importance of the waveform design and diversity (WDD) paradigm [2]–[6] as a means of addressing this challenge. This approach, when implemented within a cognitive radar architecture, involves alternating between two key steps: a perception stage, where the radar detects emitters within its band of interest [7,8], and an action stage, where a spectrally-shaped waveform is designed and transmitted to minimize interference with those emitters and enhance spectrum efficiency by optimizing the signal-to-interference-plus-noise ratio (SINR) [1,9]–[15].

While the open literature has mainly focused on radar detection, the present study shifts the focus to the radar imaging task. Specifically, this work proposes a cognitive inverse synthetic aperture radar (ISAR) imaging system with spectral compatibility requirements. The radar employs an electronic support measurement (ESM) system for sensing the surrounding environment and extracting relevant spectral parameters (i.e., the perception stage) [7], followed by the synthesis and transmission of a bespoke radar waveform encompassing spectral notches to avoid interfering with other radio frequency (RF) systems (i.e., the action stage). Consequently, the radar is able to perform ISAR imaging over a wide bandwidth without causing and experiencing interference from coexisting emitters.

Nevertheless, the presence of spectral notches in the transmitted waveform inevitably results in frequency domain gaps, which may eventually lead to spurious and high sidelobes in the resulting ISAR image if not adequately accounted for. To overcome this spectral-coexistence induced drawback, a compressed sensing (CS) method is then employed at the image formation stage, which allows to successfully accomplish the ISAR imaging task even in the presence of missing data in the frequency/slow-time domain [16]–[19].

To assess the performance of the proposed cognitive ISAR system, extensive numerical analyses employing a dataset of drone measurements in the frequency band $[13, 15]$ GHz and HH polarization [20,21] are reported. The results highlight the radar capability to operate within a congested spectrum environment while producing high-quality ISAR images.

The remainder of this work is organized as follows. Section II introduces the waveform design framework for spectral compatibility applications. Section III discusses the CS-based ISAR imaging technique for incomplete data in frequency/slow-time domain. In Section IV, extensive numerical analysis is reported and discussed, whereas Section V

The work of Augusto Aubry, Antonio De Maio, and Massimo Rosamilia was partially supported by the European Union under the Italian National Recovery and Resilience Plan (NRRP) of NextGenerationEU, partnership on "Telecommunications of the Future" (PE00000001 - program "RESTART").

Figure 1: An actual snapshot of the DJI Matrice 100 measured in the dataset [20].

concludes the paper[1].

II. Waveform Design for Spectral Compatibility

In this section, the problem of designing spectrally-shaped waveform is briefly introduced with reference to a cognitive radar system.

To this end, let us consider a radar operating in the presence of K emitters, each of them transmitting over a frequency band $\Omega_k = [f_1^k, f_2^k], k = 1, \ldots, K$, within the radar frequency operation range, where f_1^k and f_2^k denote the lower and upper normalized (with respect to the sampling frequency) frequencies for the kth system, respectively.

Let $c(t)$ be the baseband equivalent of the radar transmitted waveform whose complex sequence (corresponding to samples of $c(t)$ picked up at the frequency rate equal to the radar bandwidth) is $c(i),\ i = 1, \ldots, N$. To ensure spectral compatibility with the aforementioned overlaid emitters, the cognitive radar has to properly shape the spectrum of the transmitted signal to manage the amount of interfering energy produced on the shared frequency bandwidths. The average signal energy transmitted on the kth frequency band Ω_k is given by [13]

$$\frac{1}{f_2^k - f_1^k} \int_{f_1^k}^{f_2^k} S_c(f) df, \tag{1}$$

where

$$S_c(f) = \left| \sum_{n=1}^{N} c(n) e^{-j2\pi f(n-1)} \right|^2 = N |\boldsymbol{c}^\dagger \boldsymbol{p}_f|^2, \tag{2}$$

with

$$\boldsymbol{p}_f = \frac{1}{\sqrt{N}} [1, \exp(-j2\pi f), \ldots, \exp(-j2\pi(N-1)f)]^{\mathrm{T}} \tag{3}$$

the temporal steering vector tuned to the normalized frequency f. That said, by discretizing the frequency band Ω_k in N_0 discrete frequencies f_i with steps of $\Delta f = 1/N$ and denoting by

$$\boldsymbol{F}(m,n) = \frac{1}{\sqrt{N}} e^{-\frac{j2\pi(m-1)(n-1)}{N}} \tag{4}$$

the $N \times N$ Fourier matrix scaled by $1/\sqrt{N}$, a meaningful way to quantify the average energy level transmitted on Ω_k is

$$\frac{N\Delta f}{f_2^k - f_1^k} \sum_{f_i \in \Omega_k} |\boldsymbol{c}^\dagger \boldsymbol{p}_{f_i}|^2 = \frac{1}{f_2^k - f_1^k} \sum_{f_i \in \Omega_k} |\boldsymbol{c}^\dagger \boldsymbol{p}_{f_i}|^2 = \boldsymbol{c}^\dagger \boldsymbol{R}_I^k \boldsymbol{c}, \tag{5}$$

where $\boldsymbol{R}_I^k = \frac{1}{f_2^k - f_1^k} \boldsymbol{Q}_k \boldsymbol{Q}_k^\dagger$, with $\boldsymbol{Q}_k$ the submatrix of $\boldsymbol{F}$ whose columns correspond to the frequencies belonging to Ω_k.

Thus, denoting by $E_I^k,\ k = 1, \ldots, K$, the acceptable level of disturbance on Ω_k, which is related to the quality of service demanded by the kth emitter, the transmitted waveform has to comply with the constraints

$$\boldsymbol{c}^\dagger \boldsymbol{R}_I^k \boldsymbol{c} \leq E_I^k,\ k = 1, \ldots, K. \tag{6}$$

By doing so, a detailed control of the interference energy produced on each shared frequency bandwidth is enforced.

The aforementioned spectral constraints are accounted for in several waveform design algorithms described in the open literature [1,13], which could be employed at the action stage of the proposed architecture.

III. Compressed-Sensing ISAR Imaging in the Presence of Missing Data

ISAR imaging is a technique used to generate high-resolution images of moving targets. Conventional imaging processes rely on the coherent integration of received echoes over a range of aspect angles, generally resorting to Fourier-based methods. However, in the presence of missing samples in the frequency domain, for instance due to spectral notches in the transmitted waveform, the ISAR images obtained with the standard range–Doppler (RD) algorithm [22] may be distorted or exhibit a coarse resolution.

In the aforementioned context, CS represents a powerful signal processing tool capable of reconstructing signals from a limited number of measurements [23]. CS exploits the sparsity of signals, allowing for accurate reconstruction even with incomplete data. It has been successfully applied to accomplish the ISAR imaging task, yielding noteworthy improvements in the context of data reduction as well as resolution enhancement [17].

The key principle underlying CS-based ISAR imaging lies in its ability to leverage the sparsity of scatterers in the image domain. As a matter of fact, when operating at high frequencies, radar signals exhibit some degree of sparseness in a two-dimensional (2D) Fourier basis, due to the limited number of target prominent scatterers [17].

In the presence of noise, the CS approach reconstructs the ISAR image $\boldsymbol{I}$ by solving the following optimization problem

$$\begin{aligned} \hat{\boldsymbol{I}} = & \arg\min_{\boldsymbol{I}} \|\boldsymbol{I}\|_0 \\ & \text{s.t. } \|\boldsymbol{S} - \boldsymbol{\Theta}_x \boldsymbol{I} \boldsymbol{\Theta}_y\|_F^2 \leq \epsilon \end{aligned} \tag{7}$$

[1]**Notation.** Boldface is used for vectors $\boldsymbol{a}$ (lower case), and matrices $\boldsymbol{A}$ (upper case). The nth element of $\boldsymbol{a}$ and the (m,l)th entry of $\boldsymbol{A}$ are, respectively, denoted by $\boldsymbol{a}(n)$ and $\boldsymbol{A}(m,n)$. The transpose and the conjugate transpose operators are denoted by the symbols $(\cdot)^{\mathrm{T}}$ and $(\cdot)^\dagger$, respectively. For any complex number x, $|x|$ indicates the modulus of x. For any matrix $\boldsymbol{A}$, $\|\boldsymbol{A}\|_0$ and $\|\boldsymbol{A}\|_F$ denote the corresponding L0 and Frobenius norm, respectively. Finally, the letter j represents the imaginary unit (i.e. $j = \sqrt{-1}$).

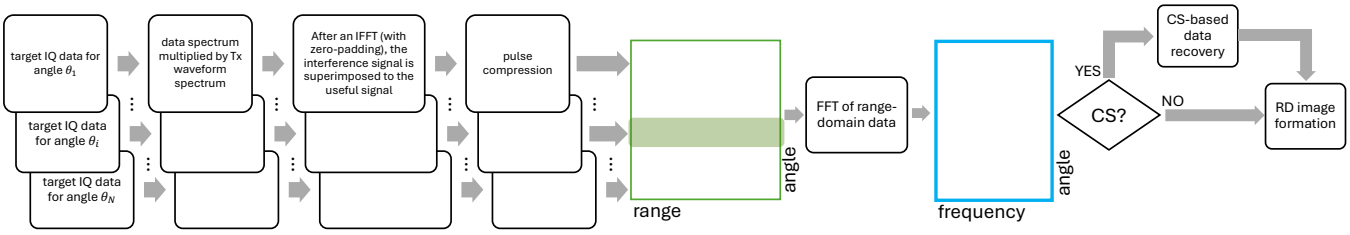

Figure 2: Flowchart depicting the simulation process employed for the numerical analysis of Section IV.

where $\boldsymbol{S}$ is the observed *incomplete* data in the slow-time/frequency domain, $\boldsymbol{\Theta}_x$ and $\boldsymbol{\Theta}_y$ are the corresponding undercomplete Fourier matrices [17], which can be computed based on the parameters of the cognitive waveform spectral notches, whereas ϵ is a user-defined parameter accounting for the noise level in the measured data.

Following the same line of reasoning as in [17], the 2D-SL0 algorithm [19] is employed to handle (7), obtaining a sparse solution consistent with the observed data.

Then, leveraging the conventional Fourier dictionaries $\boldsymbol{\Psi}_x$ and $\boldsymbol{\Psi}_y$ that perform the range compression and the cross-range compression, respectively, the corresponding reconstructed *complete-data* can be computed as

$$\hat{\boldsymbol{S}}_c = \boldsymbol{\Psi}_x \hat{\boldsymbol{I}} \boldsymbol{\Psi}_y \tag{8}$$

which allows to compute the CS-based ISAR image by means of the conventional RD algorithm [17].

It is also worth mentioning that, before the application of the aforementioned CS-based reconstruction method, a tailored pre-processing step (also accounting for the presence of possible missing data), is assumed to be carried out to compensate for the translational component in the measured signals [24,25].

IV. Numerical Analysis

In this section, the effectiveness of the proposed procedure is investigated by comparing the image obtained in the considered cognitive ISAR with those resulting from an ideal case (receiving only the useful target contribution without spectral holes) as well as a standard ISAR operating in the presence of interference. This comparison is conducted both visually and numerically by resorting to a specific quantitative metric such as the image contrast (IC).

The dataset utilized for this analysis is the one detailed in [20], which comprises measurements of various drones acquired in a semi-controlled environment across a frequency range of 8.2-18 GHz, using HH and VV polarizations, and azimuth aspect angles spanning 0-360 degrees with 0.1 degree steps and elevation close to 0 degree. In the following, the data pertaining to the DJI Matrice 100 (illustrated in Fig. 1), obtained in HH polarization with a 2 GHz bandwidth from 13 GHz to 15 GHz (considering a frequency step of 4.5 MHz) and with a target rotation of 15 degrees (with an angular resolution of 0.1 degrees), are employed for the analysis.

Four different cases are considered and compared:

- the ideal case, used as a ground truth (GT), which assumes the transmission of a standard linear frequency modulated (LFM) signal (chirp) in the absence of interference;
- the standard case, involving the transmission of standard chirp in the presence of emitters operating within the same band as the ISAR frequency range;
- cognitive case, comprising a perception stage, where the radar recognizes the presence of overlaid emitters, and an action stage, involving the synthesis (i.e., waveform design) and transmission of a tailored chirp-like signal with spectral notches in the sources frequency spectra;
- cognitive + CS case (referred to as C-CS case), wherein the CS technique proposed in [19] is applied to the data obtained in the cognitive case to reconstruct the frequency-angle data, thus allowing to counteract the potentially appearing resolution loss induced by the waveform spectral notches.

In the aforementioned scenarios, all the overlaid sources are assumed to be communication emitters.

For the aim of this analysis, the spectrum of each complex high-range-resolution (HRR) target echo signal (provided by the dataset [20] using the same pre-processing steps), for a given aspect angle θ_i (corresponding to a specific slow-time snapshot), is first multiplied by the transmitted waveform spectrum, as a first step to model (approximately) the data collected by the ISAR receiver. In the ideal and standard cases, the transmitted waveform is a standard chirp; in the other cases, it is a spectrally-shaped cognitive waveform. Subsequently, the range-domain signal, obtained following an inverse Fourier transform of the resulting spectrum, is superimposed on the interference. The resulting samples, which represent the signal measured by an actual ISAR system, undergo pulse compression with the transmitted waveform and are stored in the ith row of a range-angle data matrix. Once all the slow-time snapshots have been processed, after computing the FFT of the range-domain data, the resulting frequency-angle matrix is employed for the formation of the ISAR image using the standard RD algorithm. It should be noted that in the CS case, prior to the image formation step, the data matrix undergoes a CS-based frequency-angle data recovery algorithm. Finally, the obtained data are used for the RD image formation. The sequence of the employed steps is

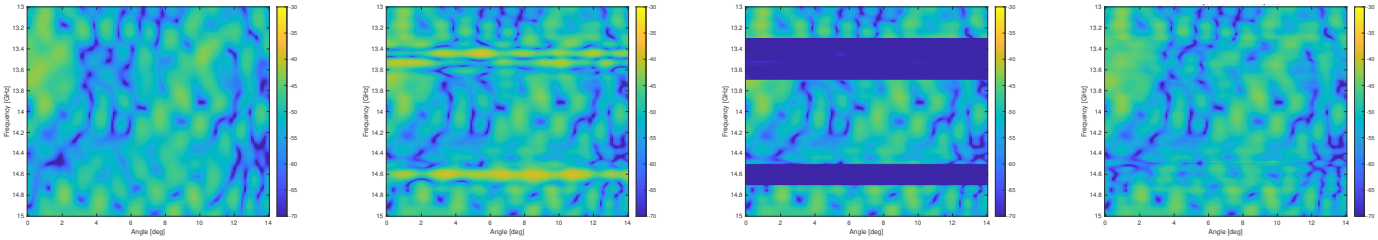

(a) (b) (c) (d)

Figure 3: Frequency-angle (dB) spectrum in the presence of two interferers. (a) GT (b) standard case (c) cognitive case (d) C-CS case.

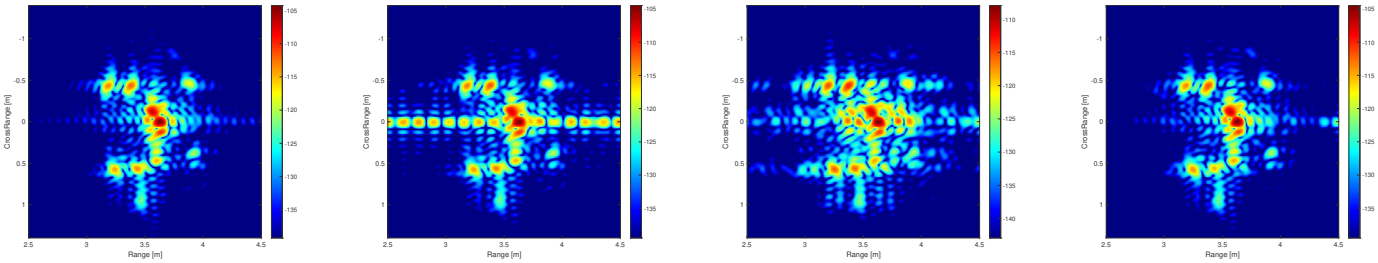

(a) (b) (c) (d)

Figure 4: ISAR image (dB) in the presence of two interferers. (a) GT (b) standard case (c) cognitive case (d) C-CS case.

illustrated in the flowchart reported in Fig. 2.

For the synthesis of the spectrally-shaped waveform to transmit in the cognitive case, a modified version of the waveform design algorithm in [13,26] is used, considering notch depths of 30 dB for the first notch and 40 dB for the second one, respectively.

The four mentioned cases are analyzed and compared across three operational scenarios, reporting the modulus (dB) of the frequency-time (i.e., frequency-angle) data, the corresponding ISAR image (obtained using the standard RD imaging procedure), and the IC value, which is a figure of merit for evaluating ISAR image quality.

The first scenario (Figs. 3 and 4) considers two communication sources, with the former operating in the range $[13.38, 13.62]$ GHz with a 240 MHz bandwidth, and the latter in the range $[14.53, 14.65]$ GHz with a 120 MHz bandwidth.

The figures clearly show that, if not properly suppressed, interfering signals introduce noticeable spurious in the resulting ISAR image (Fig. 4 (b)). Employing the cognitive approach only and down-streaming the pulse compression, the frequency-angle data results being gapped in the frequency domain (Fig. 3 (c)). The presence of these missing data is deleterious for the imaging process, resulting in high sidelobes and numerous fake scatterers (Fig. 4 (c)). Conversely, leveraging the CS technique, it is possible to reconstruct the frequency-angle data (Fig. 3 (d)) and obtain an high-quality ISAR image (Fig. 4 (d)), with negligible visual differences from the GT (Fig. 4 (a)) [17].

The second scenario (Figs. 5 and 6) involves emitters temporally varying over three time intervals:

- one emitter operating in the range $[13.45, 13.69]$ GHz with a 240 MHz bandwidth in the first interval (i.e., target aspect angles of $[0, 7]^\circ$ degrees);
- two sources, the first in $[13.38, 13.62]$ GHz with a 240 MHz bandwidth, and the second in $[14.53, 14.65]$ GHz with a 120 MHz bandwidth, in the second interval (i.e., target aspect angles of $[7, 11]^\circ$ degrees);
- one emitter in $[14.665, 14.745]$ GHz with an 80 MHz bandwidth in the third interval (i.e., target aspect angles of $[11, 15]^\circ$ degrees).

Similar to the previous scenario, the plots reveal that only in the C-CS case it is possible to obtain a faithful ISAR image of the drone. As a matter of fact, in the other cases, the interference and the missing data introduce noticeable spurious and high sidelobes in the resulting images, hindering the recognition of the drone shape.

The third scenario (Figs. 7 and 8) considers a multifunction radar that performs a number of tasks, including search, track, possible imaging of multiple targets, as well as communication activities [27,28]. Consequently, it is assumed that only 50% of the dwell time can be used for the ISAR imaging of a target, resulting in the loss of data in the slow-time dimension, in addition to those missing in the frequency domain due to the spectral notches of the cognitive waveform. This scenario further corroborates the effectiveness of the considered approach in yielding high-quality ISAR images in a contested and congested electromagnetic environment, where the use of a spectrally-shaped waveform is crucial. Furthermore, it demonstrates the potential for radar to perform additional RF operations, thereby encompassing the ISAR process within the framework of a multifunction phased array radar (MPAR) system.

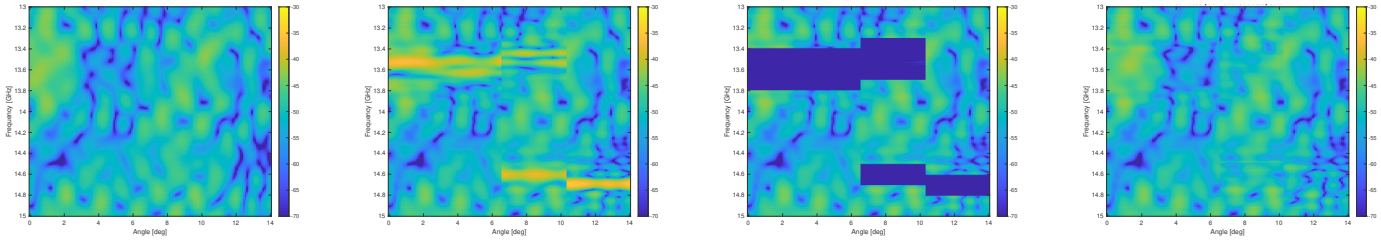

(a) (b) (c) (d)

Figure 5: Frequency-angle (dB) spectrum in the presence of different time-varying interferers. (a) GT (b) standard case (c) cognitive case (d) C-CS case.

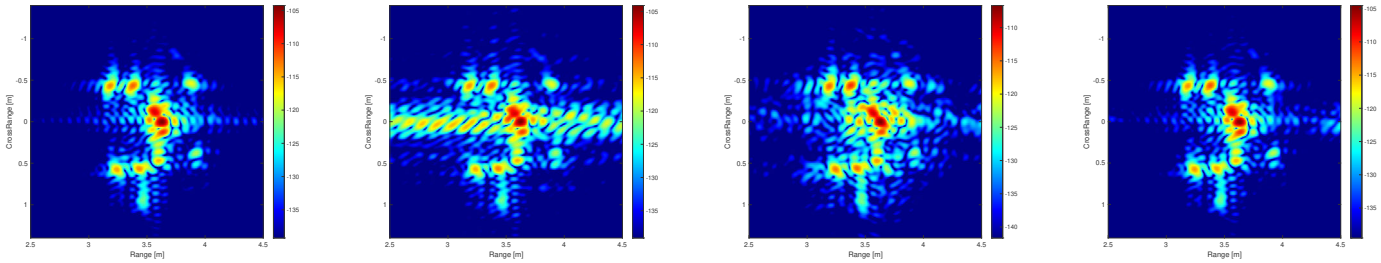

(a) (b) (c) (d)

Figure 6: ISAR image (dB) in the presence of different time-varying interferers. (a) GT (b) standard case (c) cognitive case (d) C-CS case.

Table I reports the IC values computed on the obtained ISAR images in all the analyzed scenarios. Inspection of the results reveals that the C-CS case attains the highest IC value, with values approaching those of the ground truth, pinpointing the capabilities of this method.

V. Conclusion

In this paper, a cognitive ISAR system designed to guarantee spectral compatibility with possible overlaid emitters has been proposed. To this end, the radar alternates between perception and action stages, exploiting an ESM system to recognize potential emitters within its frequency range and a tailored waveform design process to synthesize radar imaging waveforms with spectral notches used to probe the environment. In this context, the CS framework played a critical role in enabling accurate ISAR imaging by mitigating the effects of missing data both in the frequency domain, due to spectral notches in the transmitted waveform, and possibly in the slow-time dimension, due to the interrupted mode induced by higher priority tasks in a MPAR system. Extensive numerical analyses, based on drone measurements in the $[13, 15]$ GHz band, have shown that the proposed system is capable of ensuring spectral compatibility while delivering high-quality ISAR images. Several operating scenarios, including multiple communication sources, temporally varying emitters, as well as a multifunction radar operation, have been considered. The experimental results have revealed that the devised CS-based imaging method produces faithful ISAR images that are visually comparable to the ground truth, and effectively maximizes the considered numerical image quality metric.

Acknowledgment

This work was conducted during the visit of M. Rosamilia at the Microwave Integrated Systems Laboratory (MISL), University of Birmingham, U.K.. The authors would like to express their gratitude to the members of the laboratory for their invaluable support and hospitality.

References

[1] A. Aubry, V. Carotenuto, A. De Maio, A. Farina, and L. Pallotta, "Optimization theory-based radar waveform design for spectrally dense environments," *IEEE Aerosp. Electron. Syst. Mag.*, vol. 31, no. 12, pp. 14–25, 2016.

[2] S. D. Blunt et al., "Performance characteristics and metrics for intra-pulse radar-embedded communication," *IEEE J. Sel. Areas Commun.*, vol. 29, no. 10, pp. 2057–2066, 2011.

[3] G. Capraro, C. Capraro, M. Wicks, and R. Liuzzi, "Artificial intelligence and waveform diversity," in *IEMC '03 Proceedings. Managing Technologically Driven Organizations: The Human Side of Innovation and Change (IEEE Cat. No.03CH37502)*, 2003, pp. 270–274.

[4] M. Wicks and P. Antonik, "Waveform diversity in intelligent sensor systems," in *2006 IET Seminar on Waveform Diversity and Design in Communications, Radar and Sonar*. IET, 2006, pp. 1–6.

[5] F. Gini, A. De Maio, and L. Patton, *Waveform Design and Diversity for Advanced Radar Systems*. IET London, UK, 2012.

[6] G. Cui, A. De Maio, A. Farina, and J. Li, Eds., *Radar Waveform Design Based on Optimization Theory*. IET, 2020.

[7] A. Aubry, V. Carotenuto, A. De Maio, and M. A. Govoni, "Multi-snapshot spectrum sensing for cognitive radar via block-sparsity exploitation," *IEEE trans. on Signal Process.*, vol. 67, no. 6, pp. 1396–1406, 2019.

[8] A. Aubry, V. Carotenuto, A. De Maio, M. A. Govoni, and A. Farina, "Experimental analysis of block-sparsity-based spectrum sensing techniques for cognitive radar," *IEEE IEEE Trans. Aerosp. Electron. Syst.*, vol. 57, no. 1, pp. 355–370, 2021.

[9] H. He, P. Stoica, and J. Li, "Waveform design with stopband and correlation constraints for cognitive radar," in *2010 2nd International Workshop on Cognitive Information Processing*, 2010, pp. 344–349.

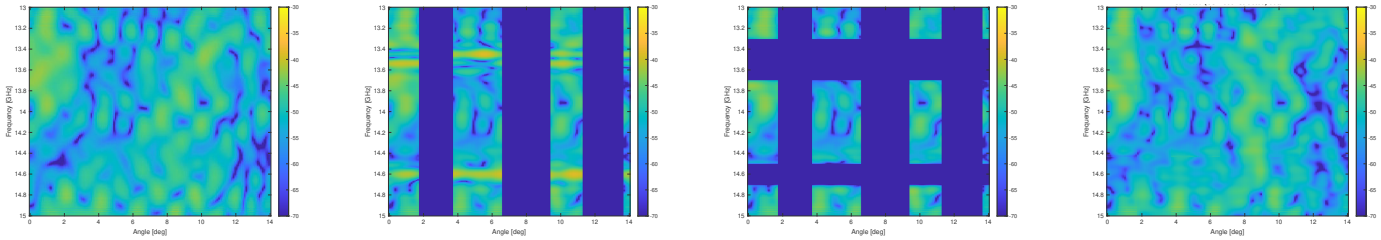

(a) (b) (c) (d)

Figure 7: Frequency-angle (dB) spectrum for a multifunction radar in the presence of two interferers. (a) GT (b) standard case (c) cognitive case (d) C-CS case.

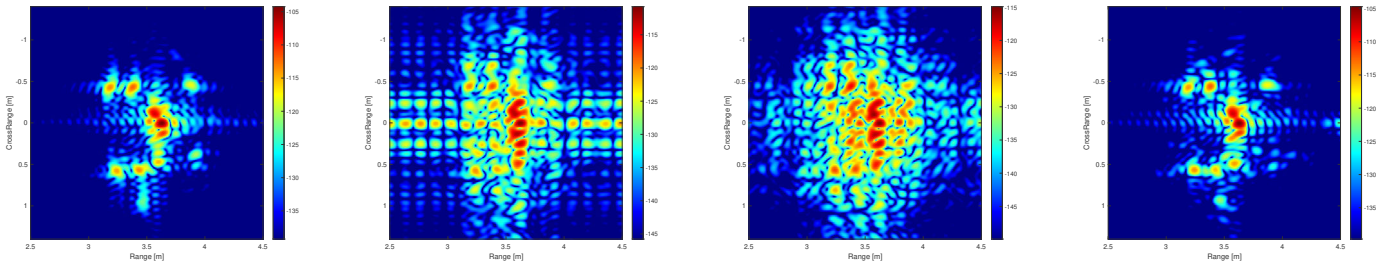

(a) (b) (c) (d)

Figure 8: ISAR image (dB) for a multifunction radar in the presence of two interferers. (a) GT (b) standard case (c) cognitive case (d) C-CS case.

Table I: IC values for the different considered scenarios and techniques.

Scenario	**GT**	**Interf. case**	**Cognitive case**	**C-CS case**
Two interferers	9.44×10^{-2}	8.39×10^{-2}	8.55×10^{-2}	$\mathbf{9.33 \times 10^{-2}}$
Time-varying interferers	9.44×10^{-2}	7.76×10^{-2}	8.24×10^{-2}	$\mathbf{8.92 \times 10^{-2}}$
MPAR in the presence of two interferers	9.44×10^{-2}	6.72×10^{-2}	7.31×10^{-2}	$\mathbf{9.00 \times 10^{-2}}$

[10] I. W. Selesnick and S. U. Pillai, "Chirp-like transmit waveforms with multiple frequency-notches," in *2011 IEEE RadarCon (RADAR)*, 2011, pp. 1106–1110.

[11] M. Piezzo, A. De Maio, A. Aubry, and A. Farina, "Cognitive radar waveform design for spectral coexistence," in *2013 IEEE Radar Conference (RadarCon13)*, 2013, pp. 1–4.

[12] R. A. Romero and K. D. Shepherd, "Friendly spectrally shaped radar waveform with legacy communication systems for shared access and spectrum management," *IEEE Access*, vol. 3, pp. 1541–1554, 2015.

[13] A. Aubry, V. Carotenuto, and A. De Maio, "Forcing multiple spectral compatibility constraints in radar waveforms," *IEEE Signal Process. Lett.*, vol. 23, no. 4, pp. 483–487, 2016.

[14] A. Farina, A. De Maio, and S. Haykin, *The Impact of Cognition on Radar Technology*, ser. Radar, Sonar & Navigation. London, U.K.: Inst. Eng. Technol., 2017.

[15] A. Aubry, A. De Maio, M. A. Govoni, and L. Martino, "On the design of multi-spectrally constrained constant modulus radar signals," *IEEE trans. on Signal Process.*, vol. 68, pp. 2231–2243, 2020.

[16] W. Qiu, E. Giusti, A. Bacci, M. Martorella, F. Berizzi, H. Zhao, and Q. Fu, "Compressive sensing–based algorithm for passive bistatic ISAR with DVB-T signals," *IEEE IEEE Trans. Aerosp. Electron. Syst.*, vol. 51, no. 3, pp. 2166–2180, 2015.

[17] S. Tomei, A. Bacci, E. Giusti, M. Martorella, and F. Berizzi, "Compressive sensing-based inverse synthetic radar imaging imaging from incomplete data," *IET radar sonar navig.*, vol. 10, no. 2, pp. 386–397, 2016.

[18] A. Bacci, D. Staglianò, E. Giusti, S. Tomei, F. Berizzi, and M. Martorella, "Compressive sensing for interferometric inverse synthetic aperture radar applications," *IET radar sonar navig.*, vol. 10, no. 8, pp. 1446–1457, 2016.

[19] A. Ghaffari, M. Babaie-Zadeh, and C. Jutten, "Sparse decomposition of two dimensional signals," in *2009 IEEE international conference on acoustics, speech and signal processing*. IEEE, 2009, pp. 3157–3160.

[20] M. Rosamilia, A. Balleri, A. De Maio, A. Aubry, and V. Carotenuto, "Radar detection performance prediction using measured UAVs RCS data," *IEEE IEEE Trans. Aerosp. Electron. Syst.*, vol. 59, no. 4, pp. 3550–3565, 2023.

[21] M. Rosamilia, A. Aubry, A. Balleri, V. Carotenuto, and A. De Maio, "Radar detection performance via frequency agility using measured UAVs RCS data," *IEEE Sensors Journal*, vol. 23, no. 19, pp. 23 011–23 019, 2023.

[22] V. Chen and M. Martorella, *Inverse synthetic aperture radar imaging: principles, algorithms and applications*. IET, 2014.

[23] A. De Maio, Y. C. Eldar, and A. M. Haimovich, *Compressed sensing in radar signal processing*. Cambridge University Press, 2019.

[24] E. Giusti, S. Tomei, A. Bacci, M. Martorella, and F. Berizzi, "Autofocus for CS based ISAR imaging in the presence of gapped data," in *Workshop on Compressive Sensng Applied to Radar (CoSeRa)*, vol. 2013. Citeseer, 2013, pp. 1–4.

[25] M. Martorella, F. Berizzi, and B. Haywood, "Contrast maximisation based technique for 2-D ISAR autofocusing," *IEE Proceedings-Radar, Sonar and Navigation*, vol. 152, no. 4, pp. 253–262, 2005.

[26] M. Rosamilia, A. Aubry, V. Carotenuto, and A. De Maio, "Non-coherent cognitive technique for frequency selective jamming," accepted for presentation at the International Conference on Radar (RADAR), Rennes, France, October 21–25, 2024.

[27] A. Aubry, A. De Maio, and L. Pallotta, "Power-aperture resource allocation for a MPAR with communications capabilities," *IEEE Trans. on Veh. Technol.*, vol. 73, no. 6, pp. 7474–7488, 2024.

[28] ——, "A priority-based scheduling scheme for search, track, and communications in mpars," *IEEE Trans. on Radar Systems*, vol. 2, pp. 471–481, 2024.

A cognitive-based ISAR system for spectral compatibility applications

Rosamilia, Massimo

2024-11-11

Rosamilia M, Aubry A, Balleri A, et al., (2024) A cognitive-based ISAR system for spectral compatibility applications. In: 2024 IEEE International Workshop on Technologies for Defense and Security (TechDefense), 11-13 November 2024, Naples, Italy

https://doi.org/10.1109/techdefense63521.2024.10863447